

Cyclotron resonance at microwave frequencies in two-dimensional hole system in AlGaAs/GaAs quantum wells

W. Pan^{a)} and K. Lai

Department of Electrical Engineering, Princeton University, Princeton, New Jersey 08544

S. P. Bayrakci and N. P. Ong

Department of Physics, Princeton University, Princeton, New Jersey 08544

D. C. Tsui

Department of Electrical Engineering, Princeton University, Princeton, New Jersey 08544

L. N. Pfeiffer and K. W. West

Bell Labs, Lucent Technologies, Murray Hill, New Jersey 07974

(Received 26 June 2003; accepted 10 September 2003)

Cyclotron resonance at the microwave frequency is used to measure the band edge mass (m_b) in the two-dimensional hole (2DH) system, confined in 30 nm quantum wells in the $\text{Al}_{0.1}\text{Ga}_{0.9}\text{As}/\text{GaAs}/\text{Al}_{0.1}\text{Ga}_{0.9}\text{As}$ heterostructures. We find that for 2DH density $p \leq 1.0 \times 10^{10} \text{ cm}^{-2}$, m_b is nearly constant, $\sim 0.35m_e$. It increases with increasing density, to $\sim 0.5m_e$ at $p = 7.4 \times 10^{10} \text{ cm}^{-2}$. © 2003 American Institute of Physics. [DOI: 10.1063/1.1623008]

It is of great interest to know the band edge mass (m_b) of the two-dimensional hole system (2DHS) in the GaAs/ $\text{Al}_x\text{Ga}_{1-x}\text{As}$ heterostructures. It determines the strength of hole-hole interaction, as well as the maximum switching speed for electronic and optical devices. Extensive experimental¹⁻⁷ and theoretical⁸⁻¹¹ investigations have been carried out to address this matter and it appears that, unlike the situation in the two-dimensional electron system where m_b is constant, m_b in the 2DHS depends strongly on sample parameters.

This intrinsic complexity of m_b in the 2DHS is due to the nonparabolic nature of the 2D valence bands, originating from the admixture of heavy hole band and light hole band. As a result, m_b strongly depends on, for example, the 2DH confining potential, its density, and, in the case of the strained-layer GaAs/ $\text{In}_x\text{Ga}_{1-x}\text{As}$ heterostructures, the built-in strain.¹² Previous experimental investigations¹⁻⁶ mostly were carried out at the 2D hole density $p > 1 \times 10^{11} \text{ cm}^{-2}$, and only recently down to $4 \times 10^{10} \text{ cm}^{-2}$.⁷ On the other hand, there is an emergent need, in recent studies of the 2D metal-to-insulator transition,¹³ to know m_b at much lower densities, for example, down to the $p \sim 10^9 \text{ cm}^{-2}$ range.

In this letter, we report the experimental results of m_b , using the cyclotron resonance (CR) technique, in the density range from as low as $p = 3.4 \times 10^9 \text{ cm}^{-2}$ to $p = 7.4 \times 10^{10} \text{ cm}^{-2}$. We find that m_b is nearly constant, $\sim 0.35m_e$ (m_e is the electron mass), when $p \leq 1.0 \times 10^{10} \text{ cm}^{-2}$, and increases with increasing 2DH density, to $\sim 0.5m_e$ at $p = 7.4 \times 10^{10} \text{ cm}^{-2}$. Results on the edge magnetoplasmon resonance are also presented.

We have investigated a total of eight samples. The typical size of each sample is about 1 mm \times 2 mm. On the surface of sample 2, disk-like mesas of diameter 250 μm were patterned by chemically etching to a depth of ~ 600

nm, shown in the inset of Fig. 2(b). All eight samples are high mobility molecular beam epitaxy (MBE)-grown GaAs/ $\text{Al}_{0.1}\text{Ga}_{0.9}\text{As}$ quantum wells (QW) of 30 nm wide, δ -doped from both sides. The detailed sample growth structure is shown in the inset of Fig. 3. Table I lists the sample parameters of the 2DH density (p), dc mobility (μ), dc relaxation time (τ_{dc}), CR relaxation time (τ_{CR}) measured at 40 GHz, as well as m_b . The 2DH density was determined by the low field Hall resistance. It is interesting to notice that at the temperature (T) of 4.2 K, μ is roughly constant, between $\sim 2 \times 10^5$ and $\sim 3 \times 10^5 \text{ cm}^2/\text{V s}$, for all eight samples, although at $T \sim 50 \text{ mK}$ it differs considerably from sample to sample, e.g., $\mu \sim 1 \times 10^6 \text{ cm}^2/\text{V s}$ for sample 1 and $\mu \sim 2.5 \times 10^5 \text{ cm}^2/\text{V s}$ for sample 8. This shows that phonon scattering is an important mechanism to limit the 2DH mobility at $T = 4.2 \text{ K}$.

Cyclotron resonance measurements at the microwave frequency (f) were performed to determine m_b . During measurement, f was fixed and the magnetic (B) field was swept. Close to resonance, the 2DHS absorbs heavily the microwave radiation power and, as a result, the sample lattice temperature rises above 4.2 K. This temperature difference is then detected by an adjacent thermometer. In the linear response regime, where all the measurements were carried out, the CR signal is proportional to the absorbed microwave power, or, in other words, the real part of the complex 2DH conductivity. Further details of our experimental technique can be found in Ref. 14.

Figure 1 shows the magnetic field dependence of the microwave absorption signal obtained at a frequency of 40 GHz and $T = 4.2 \text{ K}$ for four different samples with 2DH density ranging from 3.4×10^9 to $7.4 \times 10^{10} \text{ cm}^{-2}$. All curves display a well-defined resonance peak. The line shape of these curves can be fitted by the Drude model.¹⁵ Under this model, the real part of conductivity is given by $\text{Re}\{\sigma_{xx}\}/\sigma_0 = [1 + (\omega\tau_{CR})^2 + (\omega_c\tau_{CR})^2] / \{[1 + (\omega_c\tau_{CR})^2 - (\omega\tau_{CR})^2]^2 + 4(\omega\tau_{CR})^2\}$ (σ_0 is the static conductivity, $\omega = 2\pi f$, and τ_{CR} is the CR relaxation time), and σ_0 , m_b , and τ_{CR} are the

^{a)}Present address: Sandia National Laboratories; electronic mail: wpan@sandia.gov

TABLE I. The 2D hole density p , band edge mass m_b , dc mobility μ , dc relaxation time τ_{dc} , and the CR relaxation time τ_{CR} at the microwave frequency of 40 GHz. All quantities are measured at 4.2 K.

Sample	p (10^{10} cm $^{-2}$)	m_b (m_e)	μ (10^5 cm 2 /V s)	τ_{dc} (10^{-12} s)	τ_{CR} (10^{-12} s)
1 (01-12-99-1)	7.4	0.50	2.6	74	12
2 (12-02-98-1)	5.2	0.46	2.1	55	15
3 (12-22-98-1)	4.1	0.42	2.5	61	13
4 (10-16-98-1)	3.7	0.44	2.7	67	16
5 (10-16-98-2)	2.2	0.38	2.3	49	12
6 (01-12-99-2)	1.2	0.34	2.3	44	13
7 (01-27-99-1)	0.64	0.37	2.8	59	11
8 (02-26-99-2)	0.34	0.35	3.1	62	9

fitting parameters. A fit for sample 8 is shown. m_b deduced by this kind of fit is consistent with the values obtained from the fits illustrated in Fig. 2(a) and discussed later in the text. We have noticed that τ_{CR} is roughly five times smaller than τ_{dc} and depends on the microwave frequency (or the resonant B field B_{CR}). In Table I, we list τ_{CR} measured at 40 GHz for all the eight samples.

In Fig. 2(a), f vs B_{CR} is plotted for sample 2. For the frequencies higher than 40 GHz, clearly f shows a linear dependence on B_{CR} . A mass of $0.46m_e$ is then readily deduced from the slope of this linear relationship, according to the equation $hf = \hbar\omega_c = \hbar eB/m_b$, where ω_c is the cyclotron resonant frequency. For the frequencies lower than 20 GHz, the data points deviate from the linear dependence and the resonance is split into two branches, which merge toward a single finite value, $\omega_0 \sim 7$ GHz, at $B=0$ T. This kind of B field dependent CR is due to the coupling of the edge magnetoplasmon (EMP) mode to the cyclotron resonance mode. Consequently, the resonant frequency is modified to $\omega_{\pm} = \pm\omega_c/2 + [(\omega_c/2)^2 + \omega_0^2]^{1/2}$,¹⁶ where ω_0 is the EMP frequency at $B=0$ T, determined by the sample geometry and

2DH density. ω_+ corresponds to the upper branch for the frequencies higher than ω_0 and ω_- to the lower branch for the frequencies lower than ω_0 . In Fig. 2(b), we show the resonance of lower branch at $f=2, 5$, and 7 GHz, and of upper branch at $f=9$ GHz. One point is worth emphasizing here. Because of the coupling of EMP, fit to either the CR line shape by the classical Drude model or the data of f vs B_{CR} at $f < 20$ GHz by the linear equation, $hf = \hbar eB/m_b$, will inevitably result in a wrong value of m_b . In order to obtain the right value, it is necessary to fit the data of f vs B_{CR} according to ω_{\pm} . The dotted lines in Fig. 2(a) show such fits, including both the low frequency and high frequency parts. It results in a mass of $0.47m_e$, consistent with that obtained from the linear fit for high frequencies.

Results on m_b are listed in Table I for all eight samples and plotted in Fig. 3 as a function of 2DH density. It is clearly seen that m_b is roughly constant, $\sim 0.35m_e$, when $p \leq 1.0 \times 10^{10}$ cm $^{-2}$, and increases with increasing density, to $\sim 0.5m_e$ at $p = 7.4 \times 10^{10}$ cm $^{-2}$.

This density dependence of m_b is consistent with the picture of the nonparabolicity of 2D hole valance bands.⁸⁻¹¹ In the presence of QW confinement, the heavy hole (HH) band and light hole (LH) band split apart at the center of the Brillouin zone. Away from the zone center, the HH and LH bands admix and this gives rise to the nonparabolicity of 2DH valance bands. When density is low and the Fermi wave factor k_F is small, the nonparabolic effect is small and

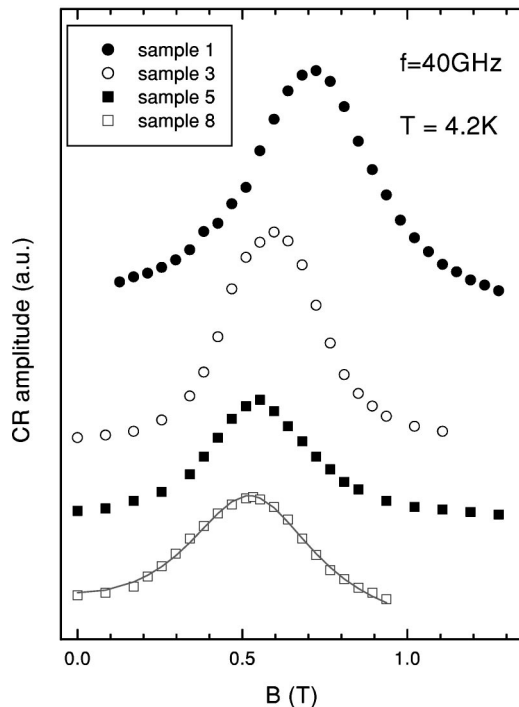


FIG. 1. Cyclotron resonance at a microwave frequency of 40 GHz and temperature of 4.2 K for samples 1, 3, 5, and 8. Curves are shifted vertically for clarity. The solid line on the data points of sample 8 is a fit according to the classical Drude model.

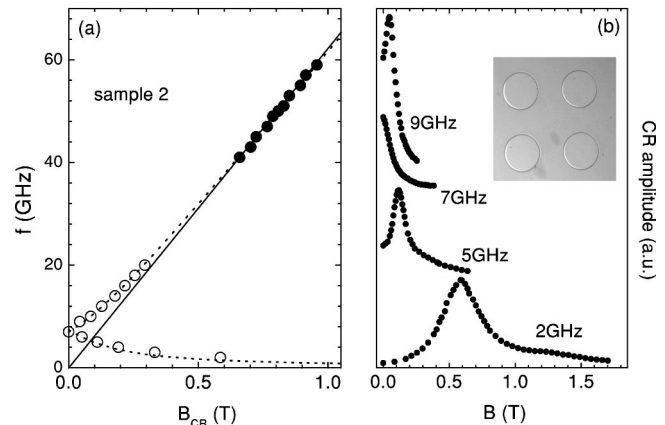


FIG. 2. Microwave frequency as a function of resonant magnetic field B_{CR} . The solid line is a linear fit to the high frequency data points. The dotted lines are fits for the data points at all frequencies, according to the equation $\omega_{\pm} = \pm\omega_c/2 + [(\omega_c/2)^2 + \omega_0^2]^{1/2}$. Figure 2(b), EMP resonance for sample 2 at the microwave frequencies $f=2, 5, 7$, and 9 GHz. The inset of Fig. 2(b) shows the disk-like mesas patterned on the surface of sample 2. The diameter of each disk is 250 μ m.

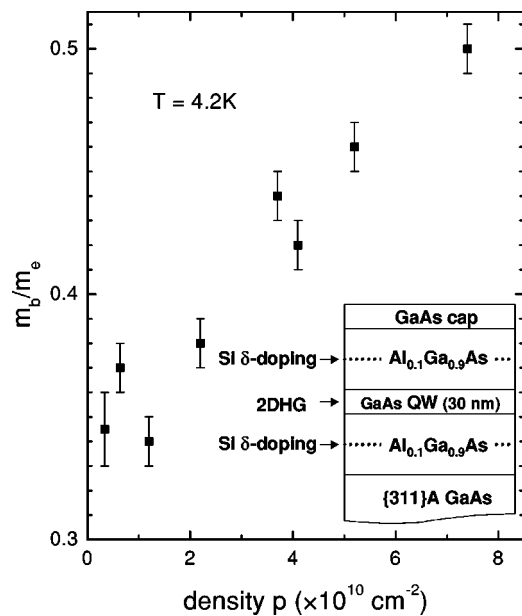


FIG. 3. 2DH band mass as a function of 2D hole density. The inset shows the schematic layer profiles for the symmetric quantum well used in the CR measurements.

the Fermi surface is nearly a circle. Consequently, m_b is expected to be constant. When density is high, the nonparabolic effect becomes important. Consequently, the Fermi circle is distorted and m_b is heavier.

Finally, from the CR measurements in a narrow QW of width 10 nm, while with other growth parameters being the same as sample 4, a lighter m_b of $\sim 0.19m_e$ is obtained. This value is about half of that measured in sample 4 of width 30 nm, and consistent with the results obtained in the QWs of similar well width in Ref. 7. The heavier m_b in wider QWs points out that the confining potential is an important parameter in determining m_b in the 2DHS. This is probably because that the separation between HH and LH bands at the center of the Brillouin zone (or $k=0$), dependent on the well width, is smaller in wider QWs. As a result, the admixture of

HH and LH bands is more severe, and consequently, m_b is heavier.

To summarize, we have measured the band edge mass of 2DHS in the symmetric GaAs/ $\text{Al}_{0.1}\text{Ga}_{0.9}\text{As}$ quantum wells of width 30 nm, using the cyclotron resonance technique at microwave frequencies. We find that m_b is nearly constant, $\sim 0.35m_e$, for 2DH density $p \leq 1.0 \times 10^{10} \text{ cm}^{-2}$ and increase with increasing density, to $\sim 0.5m_e$ at $p = 7.4 \times 10^{10} \text{ cm}^{-2}$. Edge magnetoplasmon resonance was also observed.

The authors would like to thank Wei-Li Lee for help. The work at Princeton was supported by the NSF.

- ¹H. L. Stormer and W. T. Tsang, Appl. Phys. Lett. **36**, 685 (1980).
- ²Z. Schlesinger, S. J. Allen, Y. Yafet, A. C. Gossard, and W. Wiegmann, Phys. Rev. B **32**, 5231 (1985).
- ³Y. Iye, E. E. Mendez, W. I. Wang, and L. Esaki, Phys. Rev. B **33**, 5854 (1986).
- ⁴W. Erhardt, W. Staghuhn, P. Byszewski, M. von Ortenberg, G. Landwehr, G. Weimann, L. Van Bockstal, P. Janssen, F. Herlach, and J. Witters, Surf. Sci. **170**, 581 (1986).
- ⁵Y. Iwasa, N. Miura, S. Tarucha, H. Okamoto, and T. Ando, Surf. Sci. **170**, 587 (1986).
- ⁶K. Hirakawa, Y. Zhao, M. B. Santos, M. Shayegan, and D. C. Tsui, Phys. Rev. B **47**, 4076 (1993).
- ⁷B. E. Cole, J. M. Chamberlain, M. Henini, T. Chang, W. Batty, A. Wittlin, J. A. A. T. Perenboom, A. Ardavan, A. Polisski, and J. Singleton, Phys. Rev. B **55**, 2503 (1997).
- ⁸D. A. Broido and L. J. Sham, Phys. Rev. B **31**, 888 (1985).
- ⁹U. Ekenberg and M. Altarelli, Phys. Rev. B **32**, 3712 (1985).
- ¹⁰E. Bangert and G. Landwehr, Surf. Sci. **170**, 593 (1986).
- ¹¹G. Goldoni and F. M. Peeters, Phys. Rev. B **51**, 17806 (1995).
- ¹²S. Y. Lin, H. P. Wei, D. C. Tsui, and J. F. Klem, Appl. Phys. Lett. **67**, 2170 (1995).
- ¹³See, for example, Hwayong Noh, M. P. Lilly, D. C. Tsui, J. A. Simmons, E. H. Hwang, S. Das Sarma, L. N. Pfeiffer, and K. W. West, cond-mat/0206519.
- ¹⁴Y. Matsuda, N. P. Ong, Y. F. Yan, J. M. Harris, and J. B. Peterson, Phys. Rev. B **49**, 4380 (1994); S. P. Bayrakci, Ph.D. thesis, Princeton University, 1999.
- ¹⁵G. Dresselhaus, A. F. Kip, and C. Kittel, Phys. Rev. **98**, 368 (1955).
- ¹⁶See, for example, S. J. Allen, Jr., H. L. Stormer, and J. C. M. Hwang, Phys. Rev. B **28**, 4875 (1983).